Check for updates

RESEARCH ARTICLE

REVISED Development of a systematic coarse-grained model for poly(ε-caprolactone) in melt

[version 2; peer review: 4 approved]

Petra Bačová[1], Gonzalo González Huarte[1], Vagelis Harmandaris[2-4], Sergio I. Molina[1]

[1]Departamento de Ciencia de los Materiales e Ingeniería Metalúrgica y Química Inorgánica, Facultad de Ciencias, IMEYMAT, Universidad de Cadiz - Campus de Puerto Real, Puerto Real, 11510, Spain
[2]Computation-based Science and Technology Research Center, The Cyprus Institute, 20 Constantinou Kavafi Str., Nicosia, 2121, Cyprus
[3]Institute of Applied and Computational Mathematics (IACM), Foundation for Research and Technology Hellas (FORTH), Heraklion, GR-70013, Greece
[4]Department of Mathematics and Applied Mathematics, University of Crete, Heraklion, GR-71409, Greece

v2 **First published:** 23 Sep 2025, **5**:296
https://doi.org/10.12688/openreseurope.21354.1
Latest published: 24 Dec 2025, **5**:296
https://doi.org/10.12688/openreseurope.21354.2

Abstract

Background

This study introduces a systematic coarse-graining approach to model poly(ε-caprolactone) (PCL) in its melt state. The primary goal is to provide a simple and adaptable method for creating computational models of biodegradable polymers, which can then be used to study materials with a wide range of molecular weights and compositions that are relevant to industry. This research addresses the growing need for sustainable materials across various industrial applications.

Methods

To study long polymer chains, the L-OPLS force field, an adapted version of the OPLS-AA force field, was used for atomistic simulations. The data from these simulations were first thoroughly checked against existing literature and theoretical predictions to ensure their validity. These validated atomistic configurations then became the foundation for developing the coarse-grained model.

Results

The research meticulously measured both the structural and dynamic properties of the PCL at the atomistic and coarse-grained levels. The

Open Peer Review

Approval Status ✓ ✓ ✓ ✓

	1	2	3	4
version 2 (revision) 24 Dec 2025			✓ view	
version 1 23 Sep 2025	✓ view	✓ view	? view	✓ view

1. **Tejas Shah**, The University of Texas at Dallas, Richardson, USA
Michigan State University (Ringgold ID: 3078), East Lansing, USA
2. **Dimitrios G Tsalikis**, ETH Zurich Foundation, Zürich, Switzerland
3. **Sara Ranjbareslamloo**, The University of Toledo, Toledo, USA
4. **Paola Carbone**, The University of Manchester, Manchester, UK

Any reports and responses or comments on the article can be found at the end of the article.

findings show that the model is successful at accurately reproducing key characteristics across these different levels of resolution.

Conclusions

The methodology presented in this work aims to facilitate the development of computational studies that can help optimize the properties of PCL-based materials. By doing so, it has the potential to reduce the environmental and economic impact of developing new sustainable materials.

Plain Language Summary
This article describes the development and validation of a simplified computational model for a biodegradable polymer called poly(ε-caprolactone), or PCL. PCL is a sustainable alternative to traditional plastics, but simulating its properties for industrially relevant applications, such as in tissue engineering and 3D printing, can be very computationally demanding.

To overcome these computational challenges, a "coarse-grained" (CG) model was developed. This modeling approach simplifies the system by lumping groups of chemically bonded atoms into single beads, which significantly improves computational efficiency while still capturing the material's essential properties. The model was built using a "bottom-up" methodology, where data from more detailed, fine-grained (atomistic) simulations were systematically used to derive the parameters for the reduced-resolution model.

The study found that the coarse-grained model was very successful at reproducing the structural and dynamic properties of PCL. This new methodology is intended to facilitate computational studies, which can help optimize the properties of PCL-based materials and reduce the economic and environmental impact of developing new sustainable materials.

Keywords
molecular dynamics simulations, polymer physics, systematic coarse-graining, atomistic model, poly(caprolactone)



This article is included in the Marie-Sklodowska-Curie Actions (MSCA) gateway.



This article is included in the Horizon 2020 gateway.



This article is included in the Horizon Europe gateway.



This article is included in the Polymers collection.

Corresponding author: Petra Bačová (petra.bacova@uca.es)

Author roles: Bačová P: Conceptualization, Data Curation, Formal Analysis, Funding Acquisition, Investigation, Methodology, Project Administration, Supervision, Validation, Visualization, Writing – Original Draft Preparation, Writing – Review & Editing; **González Huarte G**: Data Curation, Formal Analysis, Investigation, Validation, Visualization, Writing – Review & Editing; **Harmandaris V**: Conceptualization, Funding Acquisition, Methodology, Supervision, Writing – Review & Editing; **Molina SI**: Conceptualization, Funding Acquisition, Project Administration, Supervision, Writing – Review & Editing

Competing interests: No competing interests were disclosed.

Grant information: This project has received funding from the European Union's Horizon 2020 research and innovation programme under grant agreement No. 810660, under the Horizon Europe Marie Skłodowska-Curie grant agreement No. 101105208 and from HORIZON WIDERA-2021-ACCESS-03 (Twinning project FORGREENSOFT No. 101078989).

Copyright: © 2025 Bačová P *et al*. This is an open access article distributed under the terms of the Creative Commons Attribution License , which permits unrestricted use, distribution, and reproduction in any medium, provided the original work is properly cited.

How to cite this article: Bačová P, González Huarte G, Harmandaris V and Molina SI. **Development of a systematic coarse-grained model for poly(ε-caprolactone) in melt [version 2; peer review: 4 approved]** Open Research Europe 2025, **5**:296 https://doi.org/10.12688/openreseurope.21354.2

First published: 23 Sep 2025, **5**:296 https://doi.org/10.12688/openreseurope.21354.1

REVISED **Amendments from Version 1**

The resubmitted manuscript, which details a systematic coarse-grained model for poly (ε-caprolactone) (PCL), has been thoroughly revised and reorganized to enhance its scientific clarity, accuracy, and practical presentation for the reader.

The correct chemical name, poly(ε-caprolactone), is now consistently used throughout the title and main text, correcting the previous omission of the epsilon (ε) symbol. Furthermore, the Introduction section was restructured and rewritten. This effort was undertaken to eliminate repetitive statements and strengthen the state-of-the-art summary through the inclusion of new, relevant citations.

In the Methods section, the core procedure for developing the coarse-grained (CG) model was significantly clarified. A more explicit, step-by-step description of the Iterative Boltzmann Inversion (IBI) process is now provided, detailing how essential structural distributions were derived from all-atom simulations to successfully define and refine the simplified potentials. Minor discrepancies in the calculated density among the atomistic and the CG models were also addressed in the reply to the Reviewers, and it was clarified that the results from the CG model generally fall within the statistical error of the all-atom data.

The practical utility of the CG model was better quantified through the incorporation of a computational cost comparison. This demonstrates that the CG approach is more than 100 times faster than the all-atom simulation for the longest polymer chains investigated, representing a significant gain in efficiency. Lastly, the model's robustness was further explained, namely, its transferability to model longer polymer chains, with clarification provided on the long-chain convergence of the dynamic scaling factor. In addition, the primary atomistic model's accuracy was further supported by incorporating new data and references regarding its successful verification in aqueous (water-based) environments. Figure legends were also adjusted to improve visual clarity.

Any further responses from the reviewers can be found at the end of the article

Introduction

In today's society, industries have extremely high demands that force them to mass produce to meet these needs. In the manufacturing process, industries mostly opt for the use of plastic due to its wide variety of applications, durability and cost. However, the depletion of oil resources along with increasing environmental pollution have resulted in a global concern that has led to the search for another more sustainable approach for the environment[1].

Poly(ε-caprolactone) (PCL) is a widely recognized and extensively researched biodegradable polymer, highly valued for its ability to degrade under physiological conditions[2]. Derived from petroleum, this material is semicrystalline and hydrophobic, with key properties such as crystallinity and biocompatibility strongly dependent on its molecular weight[3]. PCL offers a unique combination of characteristics, including high solubility, a low melting point and glass transition temperature, and high compatibility in mixtures, making it a material with significant potential for applications such as tissue engineering[2] and additive manufacturing[4,5].

A fundamental understanding of PCL's properties at the molecular level is crucial for optimizing its performance in these advanced applications. While atomistic molecular dynamics (MD) simulations are powerful tools for investigating the dynamic evolution of molecular systems and condensed matter, they are often limited by accessible length and time scales. Simulating complex polymer-based materials, especially high molecular-weight entangled chains over industrially relevant scales, presents a significant challenge due to the computational cost and time constraints.

To overcome these limitations, multiscale modeling approaches are increasingly employed[6–8]. Specifically, systematic coarse-grained (CG) models are developed to reduce the resolution of the system by lumping groups of chemically bonded atoms into single beads. This allows for the simulation of larger systems over extended time periods, significantly improving computational efficiency while still capturing essential material properties[7]. The development of such CG models often follows a "bottom-up" approach, where information from more detailed, fine-grained (atomistic) simulations is systematically used to derive the parameters for the reduced-resolution models. This methodology typically involves two key steps for building a CG model: i) defining the CG mapping: This establishes the correspondence between the atomistic and the reduced resolutions, determining how atoms are grouped into CG beads; ii) defining the CG effective potentials: This involves deriving the interaction potentials for the CG beads based on the statistics obtained from the atomistic system. Techniques such as iterative Boltzmann inversion (IBI)[9] are commonly utilized to match the local structural distributions of the CG model to those of the atomistic model. This ensures that the CG model accurately reproduces the structural and, with appropriate time scaling, the dynamical properties of the underlying atomistic system.

This systematic linking of simulation methodologies across different scales is essential for quantitative prediction of polymer behavior over broad spatiotemporal scales. For PCL, all-atom molecular dynamics simulations, often employing force fields like the Optimized Potentials for Liquid Simulations All-Atom (OPLS-AA) force field[10–12], have been used to study fundamental properties such as melt density, transition temperatures and mechanical characteristics[13–15]. Yungerman *et al.*, utilized the OPLS-AA and Class II Polymer Consistent Force Field (PCFF) to investigate the properties of telechelic PCL with diacrylates as reactive functionalities[15]. Their results indicated that both PCFF and OPLS-AA were capable of describing satisfactorily the geometry of individual PCL chains in dilute and melt systems, and both force fields provided properties such as density and Young's modulus comparable to the experimental data. The articles by Di Pasquale *et al.* and Lavino *et al.* primarily employed the OPLS-AA force field in their atomistic investigation of PCL chains consisting of up to 30 repeating units within various solvent environments, specifically water-acetone mixtures[16–18]. Ezquerro *et al.* chose OPLS-AA force field over AMBER force field to model polymer melt due to its superior performance in predicting PCL's density[14].

The research specifically investigated neat PCL polymer matrices of relatively short chains containing 20 monomers, which were then blended into nanocomposite systems containing either ungrafted silica nanoparticles or silica nanoparticles grafted with polyethylene glycol. Sohrabian *et al.* also investigated a nanocoposite system, but employed COMPASS (Condensed-phase Optimized Molecular Potentials for Atomistic Simulation Studies) force-field to model the PCL matrix[19]. Recently, Nie *et al.* introduced a priori temperature rescaling method (Hybrid Iterative Boltzmann Inversion - HIBI) for coarse-graining linear PCL chains in melt with the molecular weight of 5700 g/mol[6]. The method aims to compensate for the loss of entropy by scaling up the temperature a priori and successfully reproduces structural distributions, heat capacity, and Young's modulus, however, its prediction for viscosity falls short compared to the all-atom systems[6].

The current work has as its primary objective to develop a reliable and relatively simple systematic coarse-grained model for linear PCL with the capability of being extended to experimentally relevant time and length scales. We based the model on all-atom simulations of PCL which employed OPLS-AA force field adapted for studying long chains. The atomistic data were first compared to the literature data and then the polymer chains were coarse-grained at the monomeric level. The IBI method was used to capture the structural features of the studied melts and the obtained potentials were employed to simulate CG systems.

A fundamental novelty of this work resided in the investigation of PCL chains across a wide range of molecular weights, specifically from 10 up to 125 monomers (equivalent to 1143 to 14270 g/mol). This expanded range, covering the molecular weight regime from unentangled (Rouse-like) to mildly-entangled systems, provides a more robust platform for studying the influence of chain length effects on fundamental structural and dynamical properties of PCL. Study of the chain length effects is particularly relevant for industrial applications, such as additive manufacturing (3D printing), where properties like rheological behavior (e.g., viscosity) are affected by the degree of crystallinity and thus by the molecular weight of the polymer melt. The ultimate goal is to facilitate the development of the computational approaches, which would speed up the process of tuning the properties of PCL-based materials and by doing so reducing the ecological and economical impact of the property optimization of these new generation of materials.

Methods and simulation details

In our study we employed all-atom molecular dynamics simulations to study linear chains of poly(ε-caprolactone) (PCL, see the structure in Figure 1(a)) of multiple molecular weights. The simulated systems are listed in Table 1. In order to describe the interatomic forces in the systems, two types of force fields were combined, the original OPLS-AA[10] and the modified L-OPLS[11]. More specifically, L-OPLS was used as the main source of information, since this force field is based on the parameters of OPLS-AA but was optimized for long hydrocarbon chains, as well as for alcohols and esters[11].

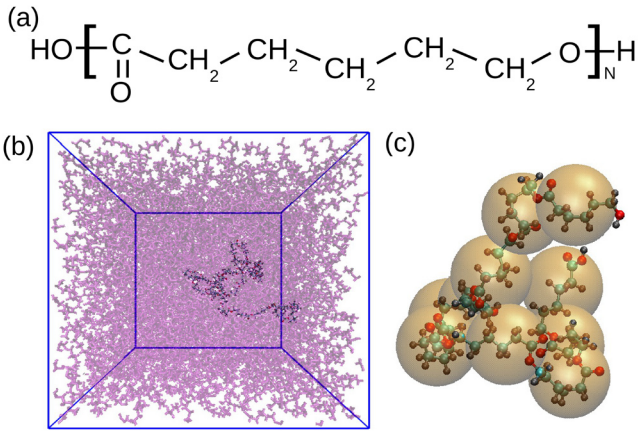


Figure 1. (**a**) Chemical structure of PCL. (**b**) Snapshot of the PCL chain of 30 monomers in melt. One chain is highlighted while the surrounding molecules are transparent for a better visibility. (**c**) Schematic illustration of the coarse-graining procedure for PCL10. Each orange sphere represents one CG unit placed in the center of mass of a monomer.

Table 1. Details about the systems under study. M_w refers to the molecular weight of the chain, N_c denotes the number of chains in the system, N is the number of monomers per chain, ρ_A refers to the density of the atomistic system and ρ_{CG} to the density of the coarse-grained system.

Label of the system	N	M_w [g/mol]	N_c	ρ_A [kg/m^3]	ρ_{CG} [kg/m^3]
PCL10	10	1143	70	928 ± 7	930±30
PCL30	30	3426	70	928 ± 4	940±20
PCL50	50	5709	70	928 ± 3	950±10
PCL100	100	11416	70	928 ± 2	939±9
PCL125	125	14270	70	928 ± 2	939±9

This optimization is in line with the objective of this work, namely, to provide a reliable and relatively simple model of PCL that could be extended to experimentally relevant time and length scales as well as to relevant molecular weights. In addition, it provides an improvement with respect to the previously published data, which relied on OPLS-AA for description of oligomeric PCL. The full set of parameters used here together with the corresponding source can be found elsewhere[20]. All the simulations were performed by open-access simulation package Gromacs[21].

Due to the lack of data on PCL modelled by L-OPLS force field, we designed the methodology as follows. In the first stage, we simulated the PCL chains in water. This step in our methodology serves as a comparative analysis with prior research. A key consideration was the lack of available studies that investigate a range of PCL's molecular weights in a molten state. Consequently, we opted to use solvent simulations to

verify our model. The radius of gyration R_g of these systems was then confronted with the published data, to corroborate the behaviour of our systems. The detailed description of the preparation of these systems, the full set of data and the results used for the comparison of R_g with the literature data are publicly available[20]. Briefly, after the preparation of a single chain molecule with the desired molecular weight (see Table 1), the chain was placed in vacuum to achieve a collapsed configuration. In continuation, so-obtained molecule was simulated in water at 300 K. The results obtained from these simulations were highly satisfactory.

The initial state of systems in melt was composed of the partially collapsed chains (see the description in ref. 20 for more information about the preparation of these chains). 70 polymer chains were randomly placed in a simulation box, big enough to avoid overlaps. The density was then adjusted by performing a short simulation at 50 bar. This preparation process is similar to the process published in ref. 22 and is used to remove gaps between chains and obtain a homogeneous density. The systems were then equilibrated in a similar way as published in ref. 23. Briefly, the systems were first equilibrated at 600 K, then they were cooled down to 500 K and then equilibrated at this temperature. The length of the equilibration run at each temperature depended on the chain length and the radius of gyration was monitored as an indicator of the equilibrated structure. Before the production run, a run of 100 ns was performed applying the same conditions as the production run. Namely, the PME method was used for the calculation of the electrostatic interactions, the velocity rescaling with a stochastic term was applied to maintain the temperature at 500 K and the Parrinello-Rahman barostat kept the pressure at 1 bar. The time step was 2 fs and the bonds containing hydrogens were constrained by the LINCS algorithm[24]. The atomistic production run was 400 ns long for chain lengths of $N = 10 - 100$ and 600 ns long for PCL125. All runs, the equilibration runs and the productions runs, are publicly available[25]. The coarse-grained simulations were performed at constant temperature of 500 K and constant pressure of 1 bar, using Nosé-Hoover thermostat and the Parrinello-Rahman barostat. The time step was 5 fs and the bonds were constrained by the LINCS algorithm[24]. The coarse-grained simulations are also publicly available[26].

Results and discussion

Polymer chains in melt typically exhibit dense and homogeneous packing, where monomers are isotropically surrounded (see also Figure 1(b)) and long-range intermolecular forces are effectively screened. This screening behavior in the melt state, where chains "screen" each other from long-range forces, causes the chain to statistically behave like an ideal chain without the excluded volume effect. This leads to a particular theoretical scaling of fundamental structural properties with the number of monomers in the chain and since in the validation step we focused on confronting the results from the atomistic model with systems in solution, in what follows we focus on confirming this theoretical assumption in melt for both atomistic and coarse-grained model derived systematically from the atomistic configurations.

In the first place, to characterize the polymer's local structure, monomer distribution functions were calculated directly from the atomistic simulation data. These distributions, encompassing bond lengths, angles, dihedrals, and monomeric radial distribution functions, served as critical target data for the subsequent coarse-graining procedure. In this procedure, the atoms were grouped into "super-atoms" or beads. More specifically, in our case each bead represented one monomer, i.e., the internal beads of the chain consisted of 18 atoms and the terminal ones of 19 and 20, due to the presence of the carboxyl and hydroxyl groups at the extremes (see also Figure 1(a)). The centre of the bead was then placed in the centre of mass of each monomer. One example of such a coarse-graining procedure is shown in Figure 1(c).

The monomer distribution functions measured from the atomistic simulations are shown in Figure 2 together with the sketch of the measured internal geometrical parameters. Considering the calculation of the non-bonded radial distribution function, note that the short-range intramolecular contributions were excluded, since those short-range interactions are intended to be described by the bonded potentials. More specifically, the exclusion was defined by the number of bonds separating two beads (i.e., CG units) in a chain. In our case, only the intramolecular distances among beads placed more than 3 bonds away from each other are included in the radial distribution function.

Despite covering a wide range of molecular weights, no significant differences in these distributions across studied PCL chains were found. This observed consistency in local structural features, regardless of the overall chain length, implies that the immediate chemical environment and inherent conformational flexibility of the PCL monomer are largely independent of the macroscopic chain size in the melt. This independence significantly simplifies the development of coarse-grained models, as a potential derived from shorter oligomers can reliably be applied to longer chains for these specific local properties, forming a robust basis for bottom-up polymer modeling.

In continuation, we applied Iterative Boltzmann Inversion (IBI), as one of the most powerful methods used to derive effective mesoscale potentials from atomistic simulations[9]. We followed closely the method published elsewhere[8], therefore we will only summarize briefly the main concepts. The coarse-grained (CG) potentials were generated in a two-stage process, beginning with an Initial Direct Boltzmann Inversion to convert the target atomistic distributions into initial estimates of the potentials. These potentials were then iteratively refined using the IBI method. The refinement was typically structured sequentially: bonded, angular, dihedral, and non-bonded potentials were tuned one after the other in cycles, in this given order. Before the pressure correction, all the contributions were also tuned at the same time. The convergence of the Iterative Boltzmann Inversion is quantified by defining a norm as the integral of the absolute difference between the target and the current step's unnormalized distributions. To ensure consistent scaling across all components, each distribution is first normalized such

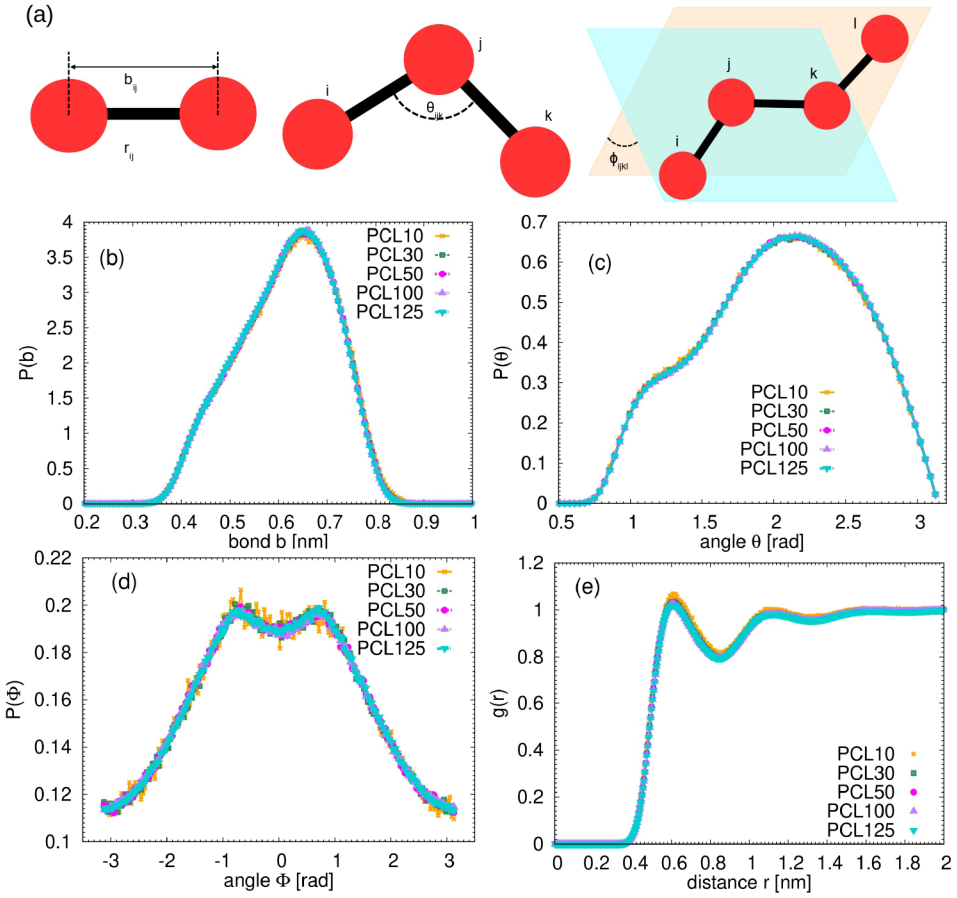


Figure 2. (**a**) Schematic illustration of the bonded interactions and the parameters plotted in the monomeric distributions (**b**–**e**) calculated from the atomistic simulations. Each bead represents one single monomer. (**b**) Distribution of the bond length between monomers. (**c**) Distribution of the angles between monomers. (**d**) Distribution of the dihedrals between monomers. (**e**) Monomeric radial distribution function for the studied systems.

that the target distribution's integral equals unity. The overall convergence norm is then calculated as the mean of the norms from all distinct contributing potentials. IBI iterations stops when this mean norm drops below a set tolerance, or when the improvement between successive steps falls below a specified small percentage. In our IBI procedure, the maximum number of iterations for each potential contribution (bonded, angular etc.) was 20. Each CG simulation within an iteration was run for up to 1500000 steps.

Figure 3 illustrates the results of the IBI procedure in comparison to the target atomistic data, which were chosen to be the data from the longest simulated polymers, PCL125. The notable agreement observed between the IBI curves and the target data across all distributions confirms that such a simple and versatile method is capable of accurately reproducing the structural characteristics derived from atomistic simulations throughout the entire studied molecular weight range.

Once ensuring that the sampled distributions achieved good agreement with the target data obtained from atomistic simulations, the derived potentials were subsequently utilized to simulate the coarse-grained (CG) systems. It is noteworthy that the reduction in the system's degrees of freedom achieved through the CG methodology directly results in a significant enhancement of computational efficiency. Specifically, a comparative performance analysis of the atomistic and CG simulations for the longest chain, PCL125, demonstrated a speed-up factor exceeding 100. This performance metric was established using a computational cluster configured with four Intel(R) Xeon CPUs E5606 @ 2.13 GHz.

In what follows we present structural analysis of both atomistic and coarse-grained systems to demonstrate that our simple methodology renders consistent results at atomistic as well as at the mesoscale.

One important measure of the internal molecular structure is the plot of internal distances, R_n^2/n, as a function of the separation n along the chain. When measured among pairs of atoms along the atomistic backbone, this quantity is directly related to the characteristic ratio C_n (or C_∞), which serves as a crucial measure of a polymer chain's intrinsic flexibility or

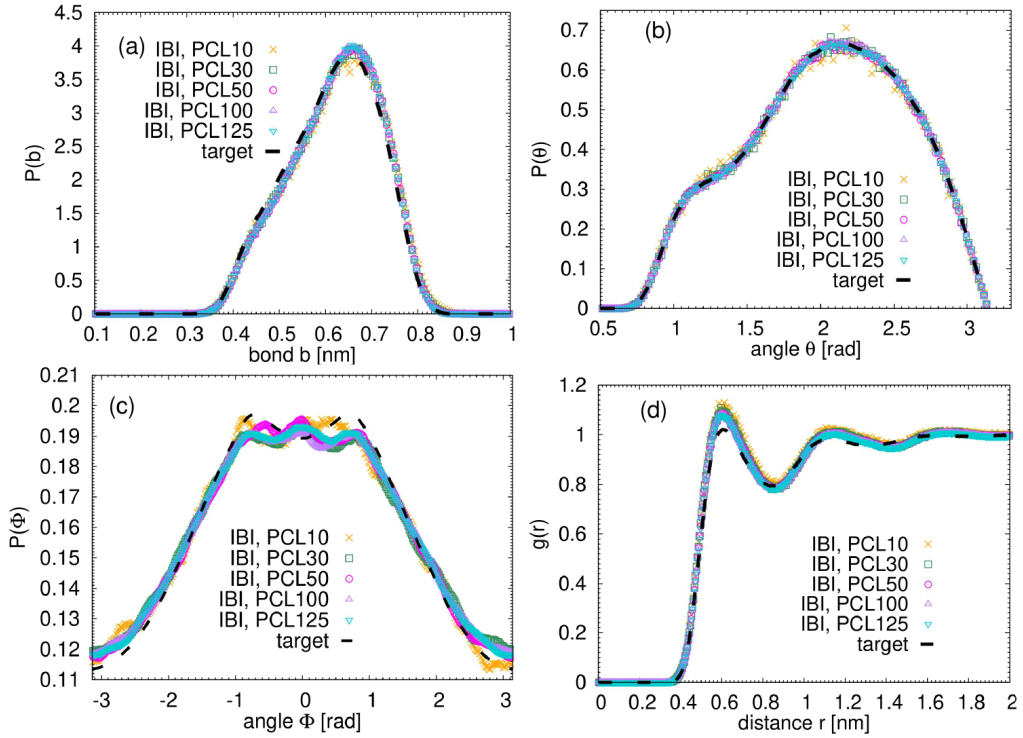


Figure 3. Results of the IBI procedure. Each bead represents one single monomer. (**a**) Distribution of the bond length between monomers. (**b**) Distribution of the angles between monomers. (**c**) Distribution of the dihedrals between monomers. (**d**) Monomeric radial distribution function for the studied systems. The dashed line represents the data from the atomistic simulation of PCL125.

extension in its unperturbed state. The C_n calculated directly from the atomistic simulations is shown in Figure 4. The characteristic ratio C_n is defined as $C_n = \langle R_n^2 \rangle / (nb_A^2)$, where $\langle R_n^2 \rangle$ is the mean squared distance between atoms, n represents the separation (of the atoms) along the chain backbone, and b_A is the average bond length in the atomistic simulations. In Figure 4 the maximum separation equals to $n_{max} = 7N - 1$, where N is the number of monomers in the chain. The value of C_n changes with n. As n gets very large, C_n approaches a maximum value, which we call C_∞. The value of C_∞ visually estimated from the plateau at long n in Figure 4 is $C_\infty \approx 5$. This estimated value is in good agreement with the previously published experimental results (C_∞ = 3.9–6[27–30]) and with the theoretical estimation from the rotational isomeric state calculations ($C_\infty = 4.1 - 4.5$[31]).

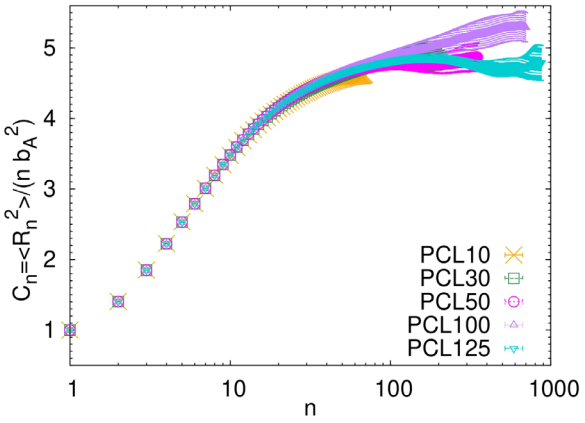


Figure 4. Characteristic ratio C_n as a function of the distance between atoms along the backbone of the atomistic chains.

In Figure 5(a) the internal distances, R_n^2/n are shown as a function of the separation n along the chain for studied PCL systems. Note that in this case, in order to be able to compare the atomistic and CG systems, n denotes the separation of the monomers (i.e., the difference in their indices) and not of the atoms. Giving the connection between the internal distances and the characteristic ratio, the differences in R_n^2/n in Figure 5(a) reflect the differences in chain stiffness. As depicted in the figure, the value of R_n^2/n generally increases with increasing separation n. For longer PCL chains, particularly those with a higher number of monomers (e.g., PCL100 and PCL125), the function demonstrates a tendency to reach a plateau at larger n values. For n equal to the number of monomers N, R_n^2 represents the squared value of the average chain span, i.e., the end-to-end distance R_e^2. The visual agreement between the atomistic and coarse-grained results in Figure 5(a) is particularly good for PCL10, and PCL30, which highlights the

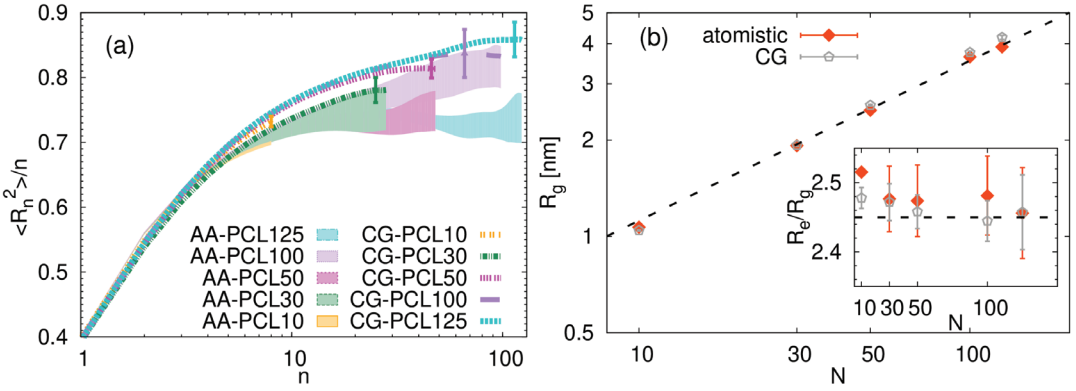


Figure 5. (**a**) Monomer internal distances as a function of the separation *n* between monomers, for the atomistic (shaded area) and CG systems (lines). The largest error bars for the CG systems are also plotted. (**b**) Radius of gyration as a function of the number of monomers, *N*. The inset shows the ratio of the end-to-end distance, R_e, to the radius of gyration, R_g. The dashed line in both cases represent the theoretical prediction, namely $R_g \sim N^{0.5}$ and $R_e/R_g = \sqrt{6}$. The error bars were calculated by the standard block method, using 4 blocks of simulation data.

consistent representation of these internal distances across different simulation resolutions. For longer chains, the CG model seems to overestimate the chain stiffness, leading to higher values of the plateau at high values of *n*. This deviation of larger-scale dimensions is attributed to the fact, that while IBI performs very well at reproducing local structural correlations, it often struggles to accurately capture larger-scale, long-range properties of polymer chains. The phenomenon is not inherent to IBI and was reported in various studies dealing with the coarse graining[8,32].

Figure 5(b) presents the radius of gyration R_g as a function of the number of monomers N for both the atomistic and coarse-grained representations of PCL. Our analysis of the atomistic data for R_g reveals a clear upward trend with increasing number of monomers, consistent with theoretical scaling predictions for polymers in the melt, namely $R_g \sim N^{0.5}$. This finding is important as it confirms that our atomistic models accurately capture the unperturbed conformational state of PCL in a dense environment.

When examining the coarse-grained results for R_g, we observe that these values for chains with $N > 30$ are generally above those obtained from the atomistic simulations for the same chain lengths. This outcome is in line with slightly more stretched character of these CG chains in comparison to their atomistic analogues observed in Figure 5(a). Despite the quantitative differences, the CG R_g values seem to maintain a similar scaling trend with N as their atomistic counterparts, indicating that the coarse-graining procedure successfully preserves the fundamental chain-length dependence of structural dimensions.

The inset of Figure 5 provides further insight into the conformational characteristics by illustrating the ratio of the end-to-end distance and the radius of gyration, R_e/R_g. For ideal chains, this ratio is theoretically $R_e/R_g = \sqrt{6}$. Our atomistic PCL chains in melt show R_e/R_g ratio that approaches this theoretical ideal value as chain length increases, more specifically, the theoretical value is reached for $N > 30$. The CG models also reflect this trend, although minor deviations from the atomistic data are present.

Figure 6(a) presents the asphericity distribution functions for the studied chains. The asphericity quantifies the shape of the molecules and is measured in simulation by calculating the geometrical inertia tensor:

$$T_{\alpha\beta} = \frac{1}{2N_p^2} \sum_i^{N_p} \sum_j^{N_p} (r_{i\alpha} - r_{j\alpha})(r_{i\beta} - r_{j\beta}), \quad (1)$$

where α,β denote the Cartesian coordinates and N_p represents the total number of particles in the chains, i.e., the number of atoms in the atomistic systems and $N_p = N$ for the CG systems. The eigenvalues of $T_{\alpha\beta}$, labelled as λ_1, λ_2, λ_3, are subsequently used to estimate the asphericity parameter from the following relation:

$$a = \frac{(\lambda_2 - \lambda_1)^2 + (\lambda_3 - \lambda_1)^2 + (\lambda_3 - \lambda_2)^2}{2(\lambda_1 + \lambda_2 + \lambda_3)^2}. \quad (2)$$

The more spherical the molecule, the closer its asphericity value is to 0. The distributions in Figure 6(a) for both atomistic and CG systems are identical within the obtained accuracy, with a sole exception of PCL125 system, which appears slightly more spherical at atomistic scale. The collected data have some features of the bimodal distributions expected by the theoretical model of a chain in θ conditions[33]. The bimodal character originates from the two distinct molecular conformations present in θ state: a collapsed conformation with lower asphericity and a coil conformation. The distributions are in a perfect agreement with the data reported previously for other common unentangled synthetic polymers in melt (see the dashed line in Figure 6(a) and the Supplementary Information in ref. 34 which reports the unpublished data for refs. 8,35 and data from ref. 36) and for poly(lactic acid) in melt[34], which confirms that the used model reproduces the expected behaviour of polymers in dense environments. It is important to note that, in contrast to poly(lactic acid) (PLA)[34],

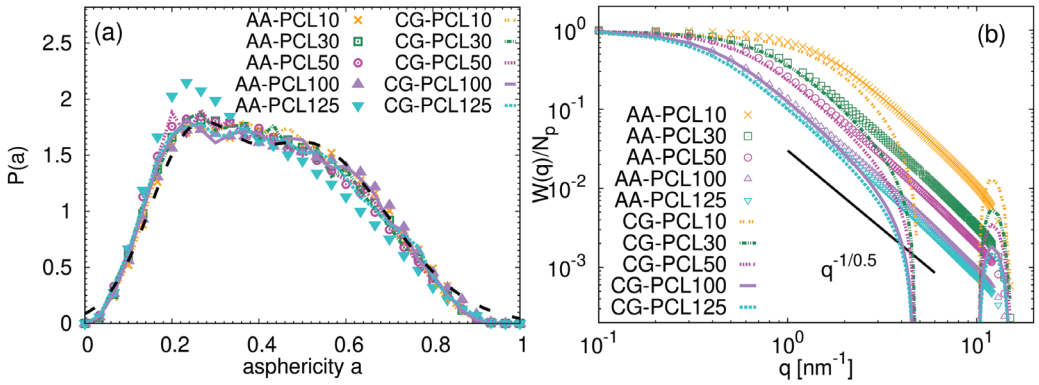


Figure 6. (**a**) Asphericity distribution for atomistic (points) and coarse-grained (lines) PCL systems. The dashed black line represents the theoretical expression reported in ref. 36 for unentangled poly(ethylene oxide). (**b**) Form factor divided by the number of particles in the molecule as a function of the q vector for atomistic (points) and coarse-grained (lines) PCL systems. The solid line indicates the ideal scaling in the intermediate range of q values.

a related sustainable polymer, we found no evidence that the asphericity parameter depends on chain length, even with the shortest PCL10 chain.

To gain further insight into the internal molecular packing, the single-molecule form factor, $W(q)$, was calculated. For a robust comparison between the coarse-grained and atomistic chains, $W(q)$ was subsequently normalized by the number of particles N_p per chain. The form factor probes the internal molecular packing at different characteristic length scales, represented by $1/q$, where q is a wave vector. Focusing on the length scales larger than the bond length (i.e., $\langle b_A \rangle \approx 0.148$ nm for atomistic and $\langle b_{CG} \rangle \approx 0.66$ nm for CG systems) and lower than the radius of gyration, $1/b \geq q \geq 1/R_g$, data in Figure 6(b) show a perfect overlap between the CG and atomistic systems for the given chain length. In addition, within this q regime, a fractal regime $W(q) \sim q^{-1/\nu}$ is anticipated and confirmed. The determined exponent $\nu = 0.5$ is typical for ideal Gaussian chains. In line with previous findings, this observation reinforces that the chains are following their predicted behavior. It is interesting to note, that a sudden drop of $W(q)$ at $q \approx 3$ nm^{-1} and a consequent maximum at $q \approx 11$ nm^{-1} is a consequence of a spherical nature of the CG units (see e.g., ref. 37 for $W(q)$ of a compact sphere).

As also described and demonstrated above, IBI method excels at reproducing the structural distributions between coarse-grained super-atoms, matching those obtained from atomistic simulations. However, CG models often exhibit faster dynamics compared to their atomistic counterparts, due to the implicit nature of friction and the averaged degrees of freedom. To accurately reproduce the dynamical properties, it is necessary to rescale the dynamics of the CG systems, often by applying a time scaling factor that compensates for the lower monomeric friction coefficient in the coarse-grained model[38–40]. In order to obtain this factor, we calculate two dynamical properties: the characteristic time related to the rotational movement of the chain and mean squared displacement of the center of mass.

The orientational autocorrelation function of the end-to-end vector for a chain provides a hint about the terminal dynamics of the chain, i.e., about the chain relaxation at long times. This function, denoted as $C(t)$, quantifies the temporal correlation of the chain's end-to-end vector orientation and is defined as:

$$C(t) = \frac{\overrightarrow{R_e}(t_0 + t) \cdot \overrightarrow{R_e}(t_0)}{|\overrightarrow{R_e}(t_0 + t)||\overrightarrow{R_e}(t_0)|}, \quad (3)$$

where $\overrightarrow{R_e}(t + t_0)$ is the end-to-end vector of the polymer chain at time $t+t_0$, and $\overrightarrow{R_e}(t_0)$ is the end-to-end vector at the time origin t_0. The angle brackets $\langle \cdot \rangle$ denote an ensemble average.

The data on $C(t)$ collected from the atomistic and CG simulations are shown in Figure 7(a). Note that the autocorrelation functions for the CG chains are considerable slower than those of their atomistic analogues and that the time axis in the CG data was rescaled (see below).

Analysis of the decay of $C(t)$ allows for the extraction of relaxation times that govern the overall reorientation of the chain. While theoretical models like the Rouse model describe the dynamics of unentangled, short polymers, predicting an exponential decay for its Rouse modes, real polymer melts often exhibit more complex features, such as stretched exponentials, due to factors like intramolecular bond correlations, excluded volume effects, and chain stiffness. Therefore, we fitted the data with the following function:

$$f(t) = A \exp(-(t/\tau)^{\beta}) \quad (4)$$

where $A \leq 1$ is a prefactor, τ is the characteristic time (either τ_A or τ_{CG}) and β is the stretch exponent. The results obtained from this analysis for the atomistic samples are summarized in Table 2. The same procedure was repeated for the CG samples, obtaining τ_{CG} and β_{CG}. Comparing the characteristic times in Table 2, the faster dynamics in CG systems is corroborated. Comparing the stretch exponents and the data overlap in Figure 7, it is clear that the $C(t)$ functions for CG chains exhibit

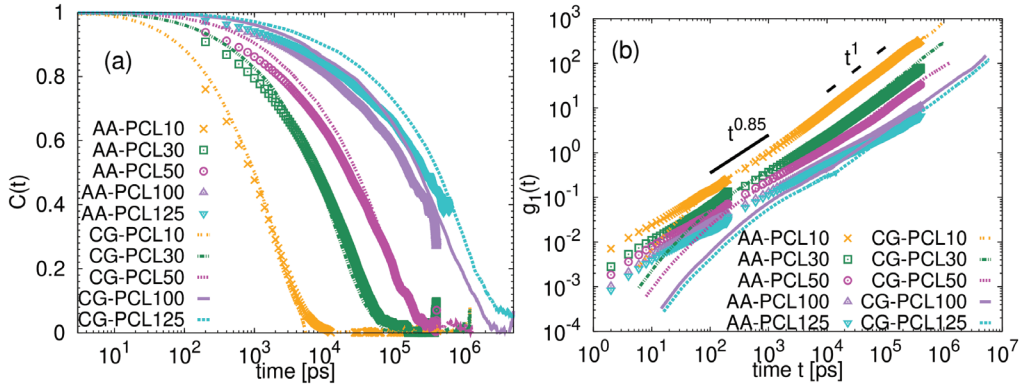


Figure 7. (**a**) Correlation function $C(t)$ of the end-to-end vector as a function of time for all simulated systems. (**b**) Mean squared displacement of the center of mass of the chains (in nm^2) as a function of time. Lines correspond to the CG systems and points to the atomistic ones. The time t for the CG data in (**a**,**b**) was multiplied by the shift factor t_{CG} to match the atomistic data. The thick solid and dashed black lines in (**b**) are guides for the eye and illustrate the power laws indicated above them.

Table 2. Results of the analysis of the dynamical properties. τ and β refer to the characteristic time and stretch exponent obtained from the fit of the end-to-end correlation function. Parameters labelled with *A* were obtained from the atomistic simulations and those labelled with *CG* from the CG simulations. The error bars were calculated by the standard block method using 4 blocks of simulation data. t_{CG} is the shift factor obtained as the ratio $t_{CG} = \tau_A/\tau_{CG}$. Units labelled with * are units in CG simulations, which do not correspond to the physical units.

Label of the system	τ_A [ns]	β_A	τ_{CG} [ns]*	β_{CG}	t_{CG}
PCL10	1.42±0.04	0.73±0.04	0.12±0.01	0.89±0.06	12±1
PCL30	13.5±0.7	0.65±0.04	1.1±0.3	0.67±0.05	12±3
PCL50	42±5	0.62±0.05	2.7±0.4	0.6±0.1	16±3
PCL100	350±110	0.48±0.06	12±3	0.55±0.08	29±14
PCL125	640±80	0.43±0.02	20±3.5	0.6±0.1	32±7

behavior more akin to simple exponential decay, as it can be anticipated for models with reduced degree of details. Their systematically higher β_{CG} values, relative to the β_A values of comparable molecular weight chains, lead to noticeable deviations in the $C(t)$ functions at early stages.

The scaling factor t_{CG}, essential to map the CG data and to account for differences in the friction in both types of simulations, was calculated as $t_{CG} = \tau_A/\tau_{CG}$. Note that after applying this scaling factor and rescaling the time axis in the $C(t)$ time dependence, there is an apparent visual mismatch in CG and atomistic data for PCL100 and PCL125. We attribute this to the fact that by rescaling the data by t_{CG}, i.e., by a ratio of characteristic times obtained from the stretched exponential function, the overlap should happen primarily around the time scales where $C(t) \approx 1/e$, thus around the characteristic time τ_A. Unfortunately, data from the atomistic simulations in this given time window are noisy and the rescaled CG data are expected to show a good match with the atomistic systems at the time scales not reached in our simulations.

To describe the translational dynamics, we calculated the mean squared displacement of the center of mass, $g_1(t)$:

$$g_1(t) = \frac{1}{N_c}\sum_{i=1}^{N_c}\left\langle \left|\mathbf{R}_{\mathrm{COM},i}(t_0+t) - \mathbf{R}_{\mathrm{COM},i}(t_0)\right|^2 \right\rangle \qquad (5)$$

where $\mathbf{R}_{\mathrm{COM},i}(t_0)$ is the position of the center of mass of the ith chain at time t_0. The data for the atomistic systems and the rescaled data for the CG systems are shown in Figure 7(b). At intermediate time scales, before reaching the diffusive regime, g_1 exhibits a sub-diffusive behavior very similar to

the one reported for multiple unentangled systems, $g_1 \sim t^{0.85}$[41]. Detailed analysis of the origin of this sub-diffusive motion is beyond the scope of this work, however, as described in ref. 41, it indicates that unentangled polymers do not behave as ideal chains in a uniform medium. Instead, their dynamics are intrinsically linked to interactions with their polymeric environment, acting as a "fixed-point" effect on their dynamic properties[41]. Concerning the agreement between the atomistic and rescaled coarse-grained $g_1(t)$s, as the chain length increases the time window of the perfect overlap shrinks, and particularly, for PCL100 and PCL125, the data only match at the long time scales. This is in line with our previous observation about the expected agreement at terminal times scales, i.e., in the diffusive regimes, which are in the case of the longest chains beyond the simulation time window.

In order to provide an alternative estimation of t_{CG}, we calculated the scaling factor from the g_1 data. We chose a characteristic time for the center-of-mass diffusion, t_1 as the time at which the chain diffuses its own size, i.e., at the time when $g_1(t_1) = R_g^2$. Consequently, we estimated t_{CG} as the ratio of these characteristic times in the atomistic and in the CG simulations for the given chain length, i.e., $t^{\mathrm{MSD}}{}_{CG} = t_{1,A}/t_{1,CG}$. Since only the chains with $N < 100$ reached the diffusive regime, the estimated values of $t^{\mathrm{MSD}}{}_{CG}$ are 15, 15 and 20 for PCL10, PCL30 and PCL50. Assuming that the value of the scaling factor should reach a constant value at high molecular weights[8], we used $t^{\mathrm{MSD}}{}_{CG} = 20$ for PCL100 and PCL125 to be able to plot the full set of data in Figure 8. Figure 8 shows that while this alternative estimation leads to a better apparent agreement in $g_1(t)$ for PCL10, PCL30 and PCL50 and at intermediate time scales also for PCL100 and PCL125, it overestimates the friction in rotational dynamics in CG systems with low molecular weight and $N < 100$ (see the $C(t)$ functions in Figure 8(a)).

Since our primary goal was to ensure the transferability of the CG potentials to much longer polymer chains, we rely on the fact that the dynamic scaling factor is expected to converge to a chain-length independent stable value once the chains are long enough; this asymptotic value can then be applied in future CG models for longer systems. Summarizing the observed behavior, the anticipated convergence is clearly supported by the scaling factor derived from the correlation function analysis (t_{CG}), as the values obtained for PCL100 and PCL125 are statistically indistinguishable within their estimated error bars. Consequently, the scaling factors determined for these longest simulated chains serve as the recommended, converged value for future models. In contrast, the scaling factor estimated from the MSD, $t^{\mathrm{MSD}}{}_{CG}$, was only reliably calculated for shorter chains ($N < 100$), which prevents us from confidently extrapolating its stable value to greater chain lengths.

To provide a quantitative analysis of the dynamical properties, we calculated the terminal relaxation time using the data reported in Table 2 from the following relation:

$$\tau_{\mathrm{end}} = \frac{\tau_{\mathrm{A}}}{\beta_{\mathrm{A}}} \Gamma\left(\frac{1}{\beta_{\mathrm{A}}}\right) \tag{6}$$

where Γ denotes the gamma function. The data are plotted as a function of the number of monomers in Figure 9. Note that the terminal relaxation time obtained in this way can be related to the terminal relaxation in rheological measurements. In addition, the Rouse model predicts the scaling of $\tau_{\mathrm{end}} \sim N^2$ for the unentangled linear polymers[42] while as the entangled regime is reached, a scaling of $\tau_{\mathrm{end}} \sim N^{3.4}$ is anticipated[43]. Looking at the illustrated power laws in Figure 9, it seems that the crossover between the Rouse regime and the entanglement regime occurs at chain lengths around 50 monomers. The critical molecular weight M_c, which marks the onset to the entanglement regime, is usually a multiple of the entanglement molecular weight, M_e, with M_c/M_e being between 2 and 7[44]. Having in mind the limited number of points in our study, the estimation of M_e, or the number of monomers per entanglement strand N_e is not directly possible from the plot in Figure 9.

As the estimation of crossover in Figure 9 is only visual, we proceed with a more rigorous way related to the structural

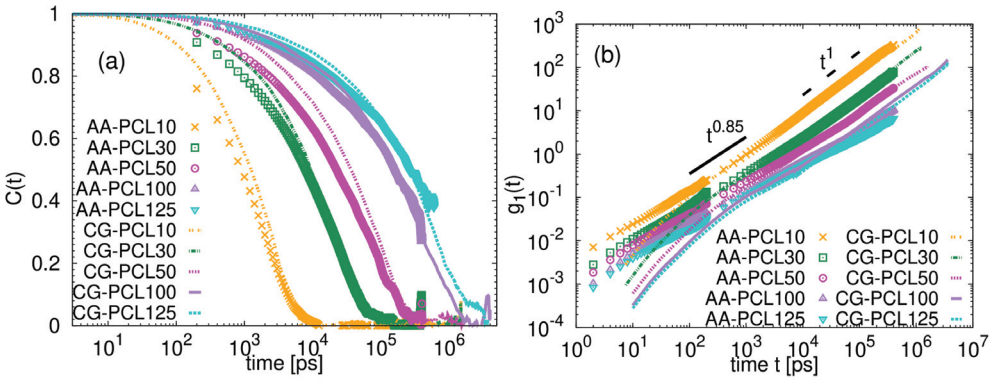


Figure 8. (**a**) Correlation function $C(t)$ of the end-to-end vector as a function of time for all simulated systems. (**b**) Mean squared displacement of the center of mass of the chains (in nm^2) as a function of time. Lines correspond to the CG systems and points to the atomistic ones. The time t for the CG data in (**a**,**b**) was multiplied by the shift factor $t^{\mathrm{MSD}}{}_{CG}$ estimated from the onset of to the diffusive regime in the mean squared displacement. The thick solid and dashed black lines in (**b**) are guides for the eye and illustrate the power laws indicated above them.

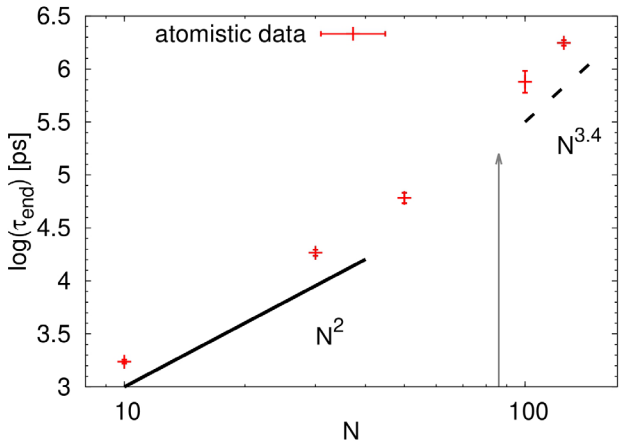


Figure 9. Terminal relaxation time τ_{end} as a function of the number of monomers *N*. The black lines are guides for the eye and indicate the scaling regimes for the Rouse model (solid line) and for the entangled regime (dashed line). The grey arrow points out to the value of $2N_e$ estimated from the packing length.

property of a system called packing length, p. Packing length relates the size of the polymer, namely its end-to-end distance R_e, to the density and the monomer mass M_w:

$$p = \frac{M_w}{\langle R_e^2 \rangle \rho N_A}, \quad (7)$$

where N_A denotes the Avogadro's constant. Considering that in our systems the density is independent of the molecular weight (see Table 1) and the scaling of R_e with N and thus with M_w is ideal, the packing length does not exhibit chain length effects. Therefore, we averaged the obtained p over the studied chain lengths, which resulted in $\langle p \rangle$ = 0.27 ± 0.01 nm. This value is close to the value of various synthetic polymers, such as polybutadiene (p = 0.21 nm) and polyisoprene (p = 0.31 nm)[44]. In addition, is in between the values reported for experimental PCL systems, namely p = 0.166 nm in ref. 27 and p = 0.315 nm in ref. 45. It is interesting to note that the calculation of the packing length from experiments is usually done through the relation $G_N \propto p^{-3}$, where G_N is the entanglement modulus[27]. Therefore, even a small difference among published G_N from the rheological experiments may cause a huge difference in the final value of p. Having estimated the value of p from simulations, we can calculate M_e such as:

$$M_e = n_t^2 \rho N_A p^3 \quad (8)$$

where n_t is a dimensionless number with a value of approximately 21[44]. The resulted value equals to M_e = 4850 g/mol, which results in $N_e \approx 43$. Assuming for simplicity that $M_c = 2M_e$, the onset to the entanglement regime would lie around $N \approx 86$ (see the arrow in Figure 9). The experimental values for M_e of PCL range between 1600 g/mol to 3900 g/mol[27,46–48], with the latest reported value of 8626 g/mol[45]. During the quantitative comparison, one should keep in mind that the experimental values were estimated from the rheological measurements and thus effects such as polydispersity, crystallization and temperature effects should be considered. Giving that our estimation of M_e relies solely on static properties, the agreement between the reported values and the one obtained in this work is satisfactory. This agreement is corroborated by the visual transition observed in Figure 9.

Conclusions

This study successfully developed and validated a systematic coarse-graining approach for poly(ε-caprolactone) (PCL) in the melt state, demonstrating its capability to quantitatively capture key structural and dynamical properties across a wide range of molecular weights.

Our atomistic simulations, combining the L-OPLS and OPLS-AA force field for a better affinity with the long chains, provided robust and consistent local structural features (bond lengths, angles, dihedrals, and radial distribution functions) that were largely independent of chain length. This consistency significantly simplified the coarse-graining process, allowing for the derivation of effective mesoscale potentials from shorter oligomers that could be reliably applied to longer chains. The Iterative Boltzmann Inversion (IBI) method proved highly effective in reproducing the structural characteristics from atomistic simulations across the entire studied molecular weight range, confirming its versatility and accuracy for local correlations.

Analysis of structural properties at both atomistic and coarse-grained levels revealed good agreement for internal distances, particularly for shorter chains (PCL10, PCL30). For longer chains, the coarse-grained model showed a tendency to overestimate chain stiffness and larger-scale dimensions, a known limitation of IBI in capturing long-range properties. Despite these deviations in chain stretching, the coarse-grained model successfully maintained the fundamental chain-length dependence of structural dimensions, as evidenced by the consistent scaling trend of the radius of gyration, R_g, with the number of monomers, N. Both atomistic and coarse-grained R_g values exhibit scaling consistent with theoretical predictions for ideal Gaussian chains in the melt ($R_g \sim N^{0.5}$), indicating that the chains adopt an unperturbed configuration. Furthermore, the ratio of end-to-end distance to the radius of gyration (R_e/R_g) for atomistic PCL chains approached the theoretical ideal value of $\sqrt{6}$ for chains with $N > 30$, a trend also reflected in the coarse-grained models. The analysis of conformational shapes, including asphericity distributions and form factors, also demonstrated good agreement between the atomistic and coarse-grained representations, further validating the structural accuracy of the coarse-grained model.

Regarding the dynamical properties, we presented results for orientational and translational dynamics of the entire chains. The coarse-grained model was appropriately time-scaled to account for the difference in the chain friction. Both dynamical properties, relaxation of the chain end-to-end vector and the mean squared displacement of the center of mass were used to extract the scaling factors. Since the dynamic scaling factor converges to a chain-length independent stable value for long chains, the

factors derived from the longest chains simulated (PCL100 and PCL125) provide the recommended, converged value for use in future long-chain models. In addition, the dependence of the terminal relaxation time of the chains on the chain length was analysed, with the aim to shed light on the transition from the unentangled to entangled behavior. Using the packing length calculated from the atomistic simulations, we estimated the entanglement molecular weight to be around 4850 g/mol, which compares reasonable well with the reported experimental values estimated from the rheological spectra and with the visual inspection of the N dependence of the terminal relaxation times from the atomistic simulations.

In summary, this work provides a reliable and relatively simple systematic coarse-grained model for linear PCL, offering a valuable tool for extending computational studies to experimentally relevant time and length scales. While the coarse-grained model accurately reproduces local structural correlations and general scaling trends, further refinement may be beneficial for precise quantitative prediction of large-scale, long-range properties in very long chains. This methodology represents a significant step towards facilitating the development of computational approaches for tuning the properties of PCL-based materials, contributing to more sustainable material development. In addition, it may serve as a first step towards quantitative predictions of rheological properties of PCL-based systems with well-controlled composition and architecture. Taking advantage of the well-defined samples in simulations, the confrontation of the simulation results with the experimentally available data and theoretical models may lead to better understanding of the structure-properties-performance relationship, without having to deal with complex features present in experimental PCL samples such as self-nucleation[46].

Ethics and consent

Ethical approval and consent were not required.

Data availability statement

Extended data

The detailed description of the preparation of the atomistic systems, the code for the preparation of a chain with a desired number of monomers, the full set of data for the simulations in water and the results used for the comparison of R_g with the literature data are publicly available[20]

(https://doi.org/10.5281/zenodo.16944033)

Underlying data

All atomistic runs are available in Zenodo (https://doi.org/10.5281/zenodo.16943800). The coarse-grained simulations with the corresponding tables for the potentials obtained from IBI procedure are also publicly available (https://doi.org/10.5281/zenodo.16944321).

Acknowledgements

This work was supported by computing time awarded from the National Infrastructures for Research and Technology S.A. (GRNET S.A.) in the National HPC facility - ARIS - under the project name ESSPO. Co-funding from UE and Junta de Andalucía (research group INNANOMAT, Ref. TEP946) are also acknowledged. Fruitful discussions with Antonis Chazirakis about the IBI algorithm are also acknowledged.

References

1. Samir A, Ashour FH, Hakim AA, *et al.*: **Recent advances in biodegradable polymers for sustainable applications.** *Npj Mater Degrad.* 2022; **6**(1): 68. **Publisher Full Text**
2. Arif ZU, Khalid MY, Noroozi R, *et al.*: **Recent advances in 3D-Printed polylactide and polycaprolactone-based biomaterials for Tissue Engineering applications.** *Int J Biol Macromol.* 2022; **218**: 930–968. **PubMed Abstract** | **Publisher Full Text**
3. Thakur M, Majid I, Hussain S, *et al.*: **Poly (ε-caprolactone): a potential polymer for biodegradable food packaging applications.** *Packag Technol Sci.* 2021; **34**(8): 449–461. **Publisher Full Text**
4. Amni C, Marwan, Aprilia S, *et al.*: **Current research in development of polycaprolactone filament for 3D bioprinting: a review.** *IOP Conf Ser Earth Environ Sci.* 2021; **926**: 012080. **Publisher Full Text**
5. Andanje MN, Mwangi JW, Mose BR, *et al.*: **Biocompatible and biodegradable 3D printing from bioplastics: a review.** *Polymers (Basel).* 2023; **15**(10): 2355. **PubMed Abstract** | **Publisher Full Text** | **Free Full Text**
6. Nie Y, Zheng Z, Li C, *et al.*: **Resolving the dynamic properties of entangled linear polymers in non-equilibrium coarse grain simulation with a *priori* scaling factors.** *Nanoscale.* 2024; **16**(13): 6548–6560. **PubMed Abstract** | **Publisher Full Text**
7. Jin J, Pak AJ, Durumeric AEP, *et al.*: **Bottom-up coarse-graining: principles and perspectives.** *J Chem Theory Comput.* 2022; **18**(10): 5759–5791. **PubMed Abstract** | **Publisher Full Text** | **Free Full Text**
8. Behbahani AF, Schneider L, Rissanou A, *et al.*: **Dynamics and rheology of polymer melts *via* hierarchical atomistic, coarse-grained, and slip-spring simulations.** *Macromolecules.* 2021; **54**(6): 2740–2762. **Publisher Full Text**
9. Reith D, Pütz M, Müller-Plathe F: **Deriving effective mesoscale potentials from atomistic simulations.** *J Comput Chem.* 2003; **24**(13): 1624–1636. **PubMed Abstract** | **Publisher Full Text**
10. Jorgensen WL, Maxwell DS, Tirado-Rives J: **Development and testing of the OPLS all-atom force field on conformational energetics and properties of organic liquids.** *J Am Chem Soc.* 1996; **118**(45): 11225–11236. **Publisher Full Text**
11. Siu SWI, Pluhackova K, Böckmann RA: **Optimization of the OPLS-AA force field for long hydrocarbons.** *J Chem Theory Comput.* 2012; **8**(4): 1459–1470. **PubMed Abstract** | **Publisher Full Text**
12. Pluhackova K, Morhenn H, Lautner L, *et al.*: **Extension of the LOPLS-AA force field for alcohols, esters, and monoolein bilayers and its validation by neutron scattering experiments.** *J Phys Chem B.* 2015; **119**(49): 15287–15299. **PubMed Abstract** | **Publisher Full Text**
13. Drenscko M, Loverde SM: **Molecular dynamics simulations of the interaction of phospholipid bilayers with polycaprolactone.** *Mol Simul.* 2019; **45**(11): 859–867. **Publisher Full Text**
14. Ezquerro CS, Aznar JMG, Laspalas M: **Prediction of the structure and mechanical properties of polycaprolactone–silica nanocomposites and the interphase region by molecular dynamics simulations: the effect of**

PEGylation. *Soft Matter.* 2022; **18**(14): 2800–2813.
PubMed Abstract | Publisher Full Text

15. Yungerman I, Starodumov I, Fulati A, *et al.*: **Full-atomistic optimized potentials for liquid simulations and polymer consistent force field models for biocompatible shape-memory poly(ε-caprolactone).** *J Phys Chem B.* 2022; **126**(21): 3961–3972.
PubMed Abstract | Publisher Full Text | Free Full Text

16. Di Pasquale N, Marchisio DL, Barresi AA, *et al.*: **Solvent structuring and its effect on the polymer structure and processability: the case of water–acetone Poly-ε-caprolactone mixtures.** *J Phys Chem B.* 2014; **118**(46): 13258–13267.
PubMed Abstract | Publisher Full Text

17. Di Pasquale N, Marchisio DL, Carbone P, *et al.*: **Identification of nucleation rate parameters with MD and validation of the CFD model for polymer particle precipitation.** *Chem Eng Res Des.* 2013; **91**(11): 2275–2290.
Publisher Full Text

18. Lavino AD, Carbone P, Marchisio D: **MARTINI coarse-grained model for poly-ε-caprolactone in acetone-water mixtures.** *Can J Chem Eng.* 2020; **98**(9): 1868–1879.
Publisher Full Text

19. Sohrabian M, Ranjbareslamloo S, Arab B, *et al.*: **Enhancing mechanical properties of PCL Biopolymers with APTES-Functionalized Bioactive Glass Nanoparticles: a molecular dynamics study.** *Computational Materials Science.* 2025; **255**: 113930.
Publisher Full Text

20. Bačová P: **PCL_Supplementary_material_systematic_CG**. 2025; (accessed September 12, 2025).
Reference Source

21. Abraham MJ, Murtola T, Schulz R, *et al.*: **GROMACS: high performance molecular simulations through multi-level parallelism from laptops to supercomputers.** *SoftwareX.* 2015; **1–2**: 19–25.
Publisher Full Text

22. Glova AD, Falkovich SG, Larin SV, *et al.*: **Poly(Lactic Acid)-based nanocomposites filled with Cellulose Nanocrystals with modified surface: all-atom molecular dynamics simulations.** *Polym Int.* 2016; **65**(8): 892–898.
Publisher Full Text

23. Christofi E, Bačová P, Harmandaris VA: **Physics-informed deep learning approach for reintroducing atomic detail in coarse-grained configurations of multiple poly(lactic acid) stereoisomers.** *J Chem Inf Model.* 2024; **64**(6): 1853–1867.
PubMed Abstract | Publisher Full Text | Free Full Text

24. Hess B, Bekker H, Berendsen HJC, *et al.*: **LINCS: a linear constraint solver for molecular simulations.** *J Comput Chem.* 1997; **18**(12): 1463–1472.
Publisher Full Text

25. Bacova P: **MD simulations of poly(caprolactone) chains of various molecular weights in melt**. 2025.
Publisher Full Text

26. Bacova P: **Coarse-grained simulations of poly(caprolactone) chains of various molecular weights in melt**. 2025.
Publisher Full Text

27. Ugartemendia JM, Muñoz ME, Sarasua JR, *et al.*: **Phase behavior and effects of microstructure on viscoelastic properties of a series of polylactides and polylactide/poly(ε-caprolactone) copolymers.** *Rheol Acta.* 2014; **53**: 857–868.
Publisher Full Text

28. Koleske JV, Lundberg RD: **Lactone polymers. II. Hydrodynamic properties and unperturbed dimensions of poly-ε-caprolactone.** *Journal of Polymer Science Part A-2: Polymer Physics.* 1969; **7**(5): 897–907.
Publisher Full Text

29. Knecht MR, Elias HG: **Zur Flexibilität aliphatischer Polyester.** *Die Makromolekulare Chemie.* 1972; **157**(1): 1–12.
Publisher Full Text

30. Jones AA, Stockmayer WH, Molinari RJ: **Nuclear magnetic resonance studies of chain dynamics in polymers.** *Journal of Polymer Science: Polymer Symposia.* 1976; **54**: 227–235.

31. Kawai A, Hamamoto N, Sasanuma Y: **Conformational characteristics and conformation-dependent properties of poly(ε-caprolactone).** *Phys Chem Chem Phys.* 2022; **24**(18): 11382–11394.
Publisher Full Text

32. Kempfer K, Devémy J, Dequidt A, *et al.*: **Development of coarse-grained models for polymers by trajectory matching.** *ACS Omega.* 2019; **4**(3): 5955–5967.
PubMed Abstract | Publisher Full Text | Free Full Text

33. Kalyuzhnyi O, Ilnytskyi JM, Holovatch Y, *et al.*: **Universal shape characteristics for the mesoscopic star-shaped polymer via dissipative particle dynamics simulations.** *J Phys Condens Matter.* 2018; **30**(21): 215101.
PubMed Abstract | Publisher Full Text

34. Bačová P, Harmandaris V, Molina SI: **Computational investigation of the structural properties of poly(lactic acid) and its stereoisomers: shape, size, and flexibility.** *Macromolecules.* 2025; **58**(16): 8572–8580.
Publisher Full Text

35. Bačová P, Li W, Behbahani AF, *et al.*: **Coupling between polymer conformations and dynamics near amorphous silica surfaces: a direct insight from atomistic simulations.** *Nanomaterials (Basel).* 2021; **11**(8): 2075.
PubMed Abstract | Publisher Full Text | Free Full Text

36. Gkolfi E, Bačová P, Harmandaris V: **Size and shape characteristics of polystyrene and poly(ethylene oxide) star polymer melts studied by atomistic simulations.** *Macromol Theor Simul.* 2021; **30**(1): 2170001.
Publisher Full Text

37. Pakula T: **Static and dynamic properties of computer simulated melts of multiarm polymer stars.** *Computational and Theoretical Polymer Science.* 1998; **8**(1–2): 21–30.
Publisher Full Text

38. Harmandaris VA, Kremer K: **Predicting polymer dynamics at multiple length and time scales.** *Soft Matter.* 2009; **5**(20): 3920–3926.
Publisher Full Text

39. Harmandaris VA, Kremer K: **Dynamics of polystyrene melts through hierarchical multiscale simulations.** *Macromolecules.* 2009; **42**(3): 791–802.
Publisher Full Text

40. Harmandaris VA: **Quantitative study of equilibrium and non-equilibrium polymer dynamics through systematic hierarchical coarse-graining simulations.** *Korea-Aust Rheol J.* 2014; **26**: 15–28.
Publisher Full Text

41. Panja D, Barkema GT, Ball RC: **Complex interactions with the surroundings dictate a tagged chain's dynamics in unentangled polymer melts.** *Macromolecules.* 2015; **48**(5): 1442–1453.
Publisher Full Text

42. Doi M, Edwards SF: **The theory of polymer dynamics**. International Series of Monographs on Physics; Oxford University Press: Oxford, 1986; **73**.
Reference Source

43. Milner ST, McLeish TCB: **Reptation and contour-length fluctuations in melts of linear polymers.** *Phys Rev Lett.* 1998; **81**: 725–728.
Publisher Full Text

44. Unidad HJ, Goad MA, Bras AR, *et al.*: **Consequences of increasing packing length on the dynamics of polymer melts.** *Macromolecules.* 2015; **48**(18): 6638–6645.
Publisher Full Text

45. Xu Y, Yu W, Zhou C: **Simultaneous slowdown of segmental and terminal relaxation of both components in dynamically asymmetric poly(ε-caprolactone)/poly(styrene-co-acrylonitrile) blends.** *Macromolecules.* 2018; **51**(18): 7338–7349.
Publisher Full Text

46. Sangroniz L, Barbieri F, Cavallo D, *et al.*: **Rheology of self-nucleated poly(ε-caprolactone) melts.** *Eur Polym J.* 2018; **99**: 495–503.
Publisher Full Text

47. Gimenez J, Cassagnau P, Fulchiron R, *et al.*: **Structure and dynamics of melt poly(ε-caprolactone) from inverse rheological calculation.** *Macromol Chem Phys.* 2000; **201**(5): 479–490.
Publisher Full Text

48. Noroozi N, Thomson JA, Noroozi N, *et al.*: **Viscoelastic behaviour and flow instabilities of biodegradable poly (ε-caprolactone) polyesters.** *Rheol Acta.* 2012; **51**: 179–192.
Publisher Full Text

Open Peer Review

Current Peer Review Status: ✔ ✔ ✔ ✔

Version 2

Reviewer Report 08 January 2026

https://doi.org/10.21956/openreseurope.23913.r66862

© **2026 Ranjbareslamloo S.** This is an open access peer review report distributed under the terms of the Creative Commons Attribution License, which permits unrestricted use, distribution, and reproduction in any medium, provided the original work is properly cited.

✔ **Sara Ranjbareslamloo**
The University of Toledo, Toledo, Ohio, USA

Approved

Competing Interests: No competing interests were disclosed.

Reviewer Expertise: Material Science Engineer/Mechanical Engineering focusing on multiscale computational modeling

I confirm that I have read this submission and believe that I have an appropriate level of expertise to confirm that it is of an acceptable scientific standard.

Version 1

Reviewer Report 17 October 2025

https://doi.org/10.21956/openreseurope.23096.r61276

© **2025 Carbone P.** This is an open access peer review report distributed under the terms of the Creative Commons Attribution License, which permits unrestricted use, distribution, and reproduction in any medium, provided the original work is properly cited.

✔ **Paola Carbone**
The University of Manchester, Manchester, England, UK

This is an interesting manuscript about the development of a coarse-grained (CG) model for poly ε-caprolactone (PCL) melts. PCL is an important polymer where a plethora of applications in particular in drug delivery but also in additive manifacturing. PCL is also difficult to simulate

especially in solutions, so having a well tested CG model is important.

The paper is clear and the methodology well explained. The results show that the CG model works well across a range of molecular weight. The quality and clarity of the figures and plots make the read smooth.

I therefore suggest publication with just a minor revision which is the following

1. For the initial testing of PCL in water, the authors might want to compare their results with the work https://doi.org/10.1021/jp505348t or
https://doi.org/10.1002/cjce.23761 whre the OPLSAA force field was used.

Is the work clearly and accurately presented and does it cite the current literature?
Yes

Is the study design appropriate and does the work have academic merit?
Yes

Are sufficient details of methods and analysis provided to allow replication by others?
Yes

If applicable, is the statistical analysis and its interpretation appropriate?
Yes

Are all the source data underlying the results available to ensure full reproducibility?
Yes

Are the conclusions drawn adequately supported by the results?
Yes

Competing Interests: No competing interests were disclosed.

Reviewer Expertise: molecular simulations of polymers

I confirm that I have read this submission and believe that I have an appropriate level of expertise to confirm that it is of an acceptable scientific standard.

Author Response 03 Dec 2025

Petra Bacova

We thank the Reviewer for a positive assessment of our manuscript. In the following we address the Reviewer's comments and describe in detail the respective changes in the new version of the manuscript.
1)*For the initial testing of PCL in water, the authors might want to compare their results with the work https://doi.org/10.1021/jp505348t or https://doi.org/10.1002/cjce.23761 where the OPLSAA force field was used.* We thank the Reviewer for highlighting these studies.

Response: We have incorporated the data from these references into the manuscript section related to the verification of our model in aqueous conditions. Furthermore, we have added these references to the Introduction of the main manuscript.

Competing Interests: No competing interests were disclosed.

Reviewer Report 17 October 2025

https://doi.org/10.21956/openreseurope.23096.r61279

© 2025 Ranjbareslamloo S. This is an open access peer review report distributed under the terms of the Creative Commons Attribution License, which permits unrestricted use, distribution, and reproduction in any medium, provided the original work is properly cited.

?

Sara Ranjbareslamloo
The University of Toledo, Toledo, Ohio, USA

Abstract and Introduction

1. Use *poly(ε-caprolactone)* consistently, not *poly(caprolactone)*.
2. 2. Abstract must include purpose, methods, key results, and significance (≤ 250 words). Current abstract meets length but lacks explicit mention of dataset DOIs.
3. In Section2 (Line 26-90) multiple sentences repeat context (e.g., biodegradable plastics, PCL sustainability). Combine to streamline flow. Rewrite lines 30–36 to one concise paragraph summarizing PCL relevance.
4. Add recent citations to strengthen background.
5. remove line-break hyphenation artifacts such as equili-brated, behav-iour.

Methods and simulation details

1. In Section 2, lines 30–33, the phrase “centers around” should be revised to “focuses on” for a more formal academic tone, and “The polymer melt behavior” should be corrected to “Polymer-melt behavior” to ensure proper compound noun usage and stylistic consistency.
2. Insert non-breaking space between number & unit (e.g., 600 K, 2 fs, 1 bar).
3. Eqs. (1–2) must italicize variables (e.g., Rg, τ, ρ). Subscripts should be upright when denoting constants.
4. Clarify whether bond/angle/dihedral distributions were directly sampled from AA MD or fitted via IBI (Line 59–61).
5. Thermostats/barostats: Justify difference between AA (velocity-rescale) and CG (Nosé–Hoover) schemes (Section 3, Line37–41).
6. Ensure equations numbered sequentially; currently Eq. (5) is cited before Eq. (4).
7. “primary” → “primarily” in time-scale overlap sentence (Sec3).

Results and Discussion

1. In the result section; “Values exhibited scaling consistent…” → “Values exhibit scaling consistent⋯” (present tense for results)
2. In the result section; Ensure subject–verb agreement in “The data shows → show.”

3. Discuss $C\infty$ discrepancy (≈ 5) – note force-field sensitivity. (explain why your computed C∞ value differs from values reported in the literature and mention that C∞ can vary depending on the force field (the atomistic potential model used).
4. Explain CG density deviation vs AA results (Result Section, line 65–67)
5. Add paragraph on scalability/transferability for higher MW chains (> 2 M_e)
6. Include a small table comparing AA vs CG simulation time per ns per chain length

Conclusions

1. In conclusion, add one sentence specifying which time-scale mapping (τ_end vs τ_MSD) is recommended for future CG predictions.
2. In conclusion avoid repetition of "facilitate computational studies to optimize PCL materials" (appears twice). Merge into one impactful closing.

References

1. Unify author initials spacing (e.g., "Bačová P et al." not "Bačová P.et.al.").

References

1. Sohrabian M, Ranjbareslamloo S, Arab B, Vaseghi M: Enhancing mechanical properties of PCL Biopolymers with APTES-Functionalized Bioactive Glass Nanoparticles: A molecular dynamics study. *Computational Materials Science*. 2025; **255**. Publisher Full Text

Is the work clearly and accurately presented and does it cite the current literature?

Yes

Is the study design appropriate and does the work have academic merit?

Yes

Are sufficient details of methods and analysis provided to allow replication by others?

Yes

If applicable, is the statistical analysis and its interpretation appropriate?

Not applicable

Are all the source data underlying the results available to ensure full reproducibility?

Yes

Are the conclusions drawn adequately supported by the results?

Yes

Competing Interests: No competing interests were disclosed.

Reviewer Expertise: Material Science Engineer/Mechanical Engineering focusing on multiscale computational modeling

I confirm that I have read this submission and believe that I have an appropriate level of expertise to confirm that it is of an acceptable scientific standard, however I have significant reservations, as outlined above.

Author Response 03 Dec 2025

Petra Bacova

We thank the Reviewer for a positive assessment of our manuscript. Some comments appear to relate to the unpublished version or formatting of the manuscript. As these issues are not present in the latest online version, we have informed the Editorial office to ensure clarity regarding the most current document. In the following we address the Reviewer's comments and describe in detail the respective changes in the new version of the manuscript.

Abstract and Introduction

1) Use poly(ε-caprolactone) consistently, not poly(caprolactone).

Response: The term was corrected.

2) *Abstract must include purpose, methods, key results, and significance (*$\leq$ 250 words). Current abstract meets length but lacks explicit mention of dataset DOIs.

Response: The dataset DOIs were omitted from the abstract in compliance with the journal's policy against including references in this section.

3) In Section2 (Line 26-90) multiple sentences repeat context (e.g., biodegradable plastics, PCL sustainability). Combine to streamline flow. Rewrite lines 30–36 to one concise paragraph summarizing PCL relevance.

Response: The introduction was rewritten. More specifically, we removed repeated statements in the paragraph describing PCL properties and we improved the state-of-the art section. *4) Add recent citations to strengthen background.* New citations were added. *5) Remove line-break hyphenation artifacts such as equili-brated, behav-iour.* The artifact is not present in the online version of the manuscript.

Methods and simulation details

1) In Section 2, lines 30–33, the phrase "centers around" should be revised to "focuses on" for a more formal academic tone, and "The polymer melt behavior" should be corrected to "Polymer-melt behavior" to ensure proper compound noun usage and stylistic consistency.

Response: The phrase "centers around" is not present in the online version of the manuscript. We kept the term "polymer melt behavior" to be consistent with the form used in most scientific and engineering contexts.

2) Insert non-breaking space between number & unit (e.g., 600 K, 2 fs, 1 bar).

Response: The error was corrected.

3) Eqs. (1–2) must italicize variables (e.g., Rg, τ, ρ). Subscripts should be upright when denoting constants.

Response: We applied these rules consistently to all equations throughout the manuscript to meet this academic standard.

4) Clarify whether bond/angle/dihedral distributions were directly sampled from AA MD or fitted via IBI (Line 59–61).

Response: The description of the IBI procedure was extended. The bond, angle, dihedral distributions as well as the radial distribution function were first calculated from the atomistic simulations (Figure 2 in the manuscript). Then the target atomistic distributions were converted into initial estimates of the potentials through direct Boltzmann inversion. In continuation, the IBI process was applied to refine the coarse-grained potentials.

5) Thermostats/barostats: Justify difference between AA (velocity-rescale) and CG (Nosé–Hoover) schemes (Section 3, Line37–41).

Response: Some of the atomistic systems were run on machines with GPUs, where the usage of Nosé-Hoover thermostat in Gromacs is discouraged. Therefore, we used temperature coupling with a velocity rescaling and a stochastic term, which ensures a proper ensemble sampling and is compatible with GPU-supported version of the simulation package. *6) Ensure equations numbered sequentially; currently Eq. (5) is cited before Eq. (4).*
Response: The artifact is not present in the online version of the manuscript.
7) primary" → "primarily" in time-scale overlap sentence (Sec3).
Response: The error was corrected.

Results and Discussion
1) In the result section; "Values exhibited scaling consistent..." → "Values exhibit scaling consistent⋯" (present tense for results)
Response: The sentence was corrected.
2) In the result section; Ensure subject–verb agreement in "The data shows → show."
Response: The sentence was corrected.
3) Discuss C∞ discrepancy (≈ 5) – note force-field sensitivity. (explain why your computed C∞ value differs from values reported in the literature and mention that C∞ can vary depending on the force field (the atomistic potential model used).
Response: We agree with the Reviewer that the characteristic ratio may vary for different force fields. The value obtained from our simulations is in excellent agreement with the experimental data and in very good agreement with the values obtained from the Rotational Isomeric State (RIS) calculations, given the accuracy of the estimation and the limitations of the RIS model. The error bar apparent from Fig. 4 is around 0.5, so having this value in mind, the characteristic ratio would be 5+/-0.5, which agrees with the RIS estimation.
4) Explain CG density deviation vs AA results (Result Section, line 65–67)
Response: Even though there are some discrepancies in the average values (about 1%), for the vast majority of systems the coarse-grained densities fall within the calculated error bars of the atomistic data. A minor exception was observed only for the PCL50 system, which exhibited a slight deviation outside this range. Given the good agreement observed across the full set of molecular weights, we consider the systematic coarse-graining procedure to be successful in reproducing the target properties.
5) Add paragraph on scalability/transferability for higher MW chains (> 2 M_e)
Response: We added a text related to the scaling factor to clarify the issue.
6) Include a small table comparing AA vs CG simulation time per ns per chain length.
Response: We included a comparison of the performance of the both models for the longest simulated chain.

Conclusions
1) In conclusion, add one sentence specifying which time-scale mapping (τ_end vs τ_MSD) is recommended for future CG predictions.
Response: A sentence about the scaling factor was added into Conclusions.
2) In conclusion avoid repetition of "facilitate computational studies to optimize PCL materials" (appears twice). Merge into one impactful closing.
Response: The artifact is not present in the online version of the manuscript.

References

1) Unify author initials spacing (e.g., "Bačová P et al." not "Bačová P.et.al.").
Response: The artifact is not present in the online version of the manuscript.

Competing Interests: No competing interests were disclosed.

Reviewer Report 14 October 2025

https://doi.org/10.21956/openreseurope.23096.r61285

© 2025 Tsalikis D. This is an open access peer review report distributed under the terms of the Creative Commons Attribution License, which permits unrestricted use, distribution, and reproduction in any medium, provided the original work is properly cited.

Dimitrios G Tsalikis
ETH Zurich Foundation, Zürich, Zurich, Switzerland

The authors utilize iterative Boltzmann inversion (IBI) to create a coarse-grained (CG) potential for polycaprolactone based on all-atom (AA) simulations. The MD simulation results using this CG potential align closely with the AA data, validating the method. The paper is well written, with a clear presentation of the findings. Overall, this research will engage the community; however, there are a few points, especially points 2-4, that need minor revision.

1. I am somewhat concerned about the predicted density from the AA simulations. Although this isn't critical for this work, I would expect oligomers (PCL 10) to have a clearly smaller density than the marginally entangled (PCL 125) due to enhanced free volume from the chain ends. Unfortunately, I couldn't find relevant experimental data. Can the authors clarify this behavior?
2. Including a brief discussion of the steps taken to obtain the CG potentials would be helpful. This would make the IBI process more reproducible for the community and increase the manuscript's visibility. For example, were all contributions tuned at the same time or one after the other, and how many refinement cycles were done for each contribution (bonds, angles, dihedrals, non-bonded)? What criteria did the authors utilize to stop refinement for each contribution?
3. Building on the previous point, during the IBI process, it is unclear whether intramolecular contributions were considered when calculating the monomeric radial distribution function. If they were, did the authors exclude first (or second or third) neighbours, since these interactions are likely captured by the bonded contributions? Is a similar exclusion applied to the corresponding CG potential?
4. Since this manuscript discusses an approach to enable community MD simulations of larger PCL chains (with molar mass> $2M_e$), which cannot be practically modelled with AA resolution due to computational cost, the authors need to demonstrate the transferability of the potential to higher MWs. This is straightforward for conformational properties. Regarding relaxation or diffusion dynamics, I understand that rescaling is necessary. But they could at least try to estimate τ^{MSD}_{CG} or at τ_{AA} through extrapolation, allowing calculations for higher MWs without conducting additional AA-MD runs.
5. And a minor point, to demonstrate to readers the power and potential of this work: I

suggest the authors include a table quantifying the computational cost for AA simulations at least for the highest molar mass examined, and compare it with the cost of the same simulations using the CG potential.

6. Lastly, another minor. I would suggest updating the legends in Figures 5a, 6ab, and 7ab to clearly distinguish between AA-MD and CG-MD without mentioning the system name twice.

Is the work clearly and accurately presented and does it cite the current literature?
Yes

Is the study design appropriate and does the work have academic merit?
Yes

Are sufficient details of methods and analysis provided to allow replication by others?
Partly

If applicable, is the statistical analysis and its interpretation appropriate?
Yes

Are all the source data underlying the results available to ensure full reproducibility?
Yes

Are the conclusions drawn adequately supported by the results?
Yes

Competing Interests: No competing interests were disclosed.

Reviewer Expertise: Multiscale modeling of soft matter.

I confirm that I have read this submission and believe that I have an appropriate level of expertise to confirm that it is of an acceptable scientific standard.

Author Response 03 Dec 2025

Petra Bacova

We thank the Reviewer for a positive assessment of our manuscript. In the following we address the Reviewer's comments and describe in detail the respective changes in the new version of the manuscript.

1. I am somewhat concerned about the predicted density from the AA simulations. Although this isn't critical for this work, I would expect oligomers (PCL 10) to have a clearly smaller density than the marginally entangled (PCL 125) due to enhanced free volume from the chain ends. Unfortunately, I couldn't find relevant experimental data. Can the authors clarify this behavior?
Response: We agree with the Reviewer, we also anticipated that the short PCL chain would exhibit lower density due to the chain end effects. However, the absence of this expected trend aligns with the lack of a molecular weight effect observed across the other static

properties reported in this manuscript. Concerning the experimental studies, investigations of low molecular weight melt of poly(caprolactone) (PCL) are scarce, and the available PCL samples are typically semicrystalline, complicating direct comparison. However, one relevant study (10.1016/j.polymer.2020.122899) reported a slightly higher melt density for low molecular weight PCL samples compared to those with high molecular weight. This observation was attributed to the positive contribution of the ester linkers to the melt density, which they suggested was due to their associated steric hindrance.

2. Including a brief discussion of the steps taken to obtain the CG potentials would be helpful. This would make the IBI process more reproducible for the community and increase the manuscript's visibility. For example, were all contributions tuned at the same time or one after the other, and how many refinement cycles were done for each contribution (bonds, angles, dihedrals, non-bonded)? What criteria did the authors utilize to stop refinement for each contribution?
Response: The tuning was sequential, starting with the bonded interactions and then with the non-bonded. Before the pressure correction, all the contributions were also tuned at the same time. The convergence of the Iterative Boltzmann Inversion is quantified by defining a norm as the integral of the absolute difference between the target and the current step's unnormalized distributions. To ensure consistent scaling across all components, each distribution is first normalized such that the target distribution's integral equals unity. The overall convergence norm is then calculated as the mean of the norms from all distinct contributing potentials. IBI iterations stops when this mean norm drops below a set tolerance, or when the improvement between successive steps falls below a specified small percentage. We extended the text related to the IBI procedure correspondingly.

3.Building on the previous point, during the IBI process, it is unclear whether intramolecular contributions were considered when calculating the monomeric radial distribution function. If they were, did the authors exclude first (or second or third) neighbours, since these interactions are likely captured by the bonded contributions? Is a similar exclusion applied to the corresponding CG potential?
Response: Considering the calculation of the potentials, the algorithm excludes short-range intramolecular contributions when calculating the non-bonded radial distribution function, since those short-range interactions are intended to be described by the bonded potentials. More specifically, the exclusion is defined by the number of bonds separating two CG atoms. In our case, the exclusion was applied up to 3 bonds away from each other. We added this information to the manuscript.

4. Since this manuscript discusses an approach to enable community MD simulations of larger PCL chains (with molar mass> 2Me), which cannot be practically modelled with AA resolution due to computational cost, the authors need to demonstrate the transferability of the potential to higher MWs. This is straightforward for conformational properties. Regarding relaxation or diffusion dynamics, I understand that rescaling is necessary. But they could at least try to estimate τ^{MSD}_{CG} or at τ_{AA} through extrapolation, allowing calculations for higher MWs without conducting additional AA-MD runs.
Response: We agree with the Reviewer on the importance of demonstrating the transferability of our potentials to higher molecular weights. We have indeed addressed the transferability for conformational properties in the manuscript. Regarding the dynamics,

while rescaling is necessary, we demonstrated that the rescaling parameter for the dynamics converges for long chains. Based on previous studies, we expect this parameter to be very close to the reported value for MWs beyond the range explicitly simulated, and thus, it should not change significantly for even longer chains. We have added a comment to the manuscript to explain this convergence.

5. And a minor point, to demonstrate to readers the power and potential of this work: I suggest the authors include a table quantifying the computational cost for AA simulations at least for the highest molar mass examined, and compare it with the cost of the same simulations using the CG potential?
Response: We added a comparison of the computational cost for one representative system.

6. Lastly, another minor. I would suggest updating the legends in Figures 5a, 6ab, and 7ab to clearly distinguish between AA-MD and CG-MD without mentioning the system name twice.
Response: We modified the figures correspondingly.

Competing Interests: No competing interests were disclosed.

Reviewer Report 03 October 2025

https://doi.org/10.21956/openreseurope.23096.r61280

© **2025 Shah T.** This is an open access peer review report distributed under the terms of the Creative Commons Attribution License, which permits unrestricted use, distribution, and reproduction in any medium, provided the original work is properly cited.

Tejas Shah
[1] The University of Texas at Dallas, Richardson, Texas, USA
[2] Biochemistry and Molecular Biology, Michigan State University (Ringgold ID: 3078), East Lansing, Michigan, USA

The manuscript presents coarse-grained modeling of poly(caprolactone) (PCL) polymers to predict melt properties using a bottom-up approach with all-atom simulations and iterative Boltzmann inversion (IBI) for coarse-graining. The topic is timely and relevant for the polymer modeling community. The manuscript can be considered for publication after the following points are addressed:

1. The overall writing is good. However, the introduction section would benefit from polishing. Some sentences are missing context, while certain statements are repeated and redundant. The authors are encouraged to refine this section to improve clarity and readability.
2. Comparison with Reported All-Atom Studies
    - Several all-atom simulation studies on PCL have been reported with shorter chains (10.1039/D4TB02789B, 10.1021/acs.jpcb.4c05368, 10.1016/j.cap.2018.07.011, 10.1021/acs.macromol.5c00158, 10.1080/07391102.2018.1541762). Did the authors compare their results with these works?

- Since CG models often deviate from experimental values due to the absence of detailed atomistic interactions, how did the authors address this limitation in their parameterization?
- If the purpose of CG was to access larger chain lengths, did the authors also perform simulations of higher molecular weight PCLs to test the robustness of the model?

3. If the entire monomer was mapped as a single bead, how were polarization effects and hydrogen-bond interactions from polar atoms accounted for in the CG model? Please clarify whether effective interactions were adjusted for this purpose.
4. The authors should clearly define how the monomer-to-monomer bond lengths, angles, and dihedrals were calculated. Were these distributions directly obtained from AA simulations, or were they imposed during the IBI process?
5. The reported CG densities show deviations compared to the all-atom model, even though the parameters were derived from AA simulations. Could the authors explain why this discrepancy occurs and what might be the source of such variation?

Is the work clearly and accurately presented and does it cite the current literature?
Yes

Is the study design appropriate and does the work have academic merit?
Yes

Are sufficient details of methods and analysis provided to allow replication by others?
Yes

If applicable, is the statistical analysis and its interpretation appropriate?
Not applicable

Are all the source data underlying the results available to ensure full reproducibility?
Yes

Are the conclusions drawn adequately supported by the results?
Yes

Competing Interests: No competing interests were disclosed.

Reviewer Expertise: Molecular Dynamics Simulations, Force Field Development, Polymer Chemistry, Biochemistry

I confirm that I have read this submission and believe that I have an appropriate level of expertise to confirm that it is of an acceptable scientific standard.

Author Response 03 Dec 2025

Petra Bacova

We thank the Reviewer for a positive assessment of our manuscript. In the following we address the Reviewer's comments and describe in detail the respective changes in the new

version of the manuscript.

1. *The overall writing is good. However, the introduction section would benefit from polishing. Some sentences are missing context, while certain statements are repeated and redundant. The authors are encouraged to refine this section to improve clarity and readability*.

We modified Introduction as requested. More specifically, we removed repeated statements in the paragraph describing PCL properties and we improved the state-of-the art section.

1. *Comparison with Reported All-Atom Studies*

-Several all-atom simulation studies on PCL have been reported with shorter chains (10.1039/D4TB02789B, 10.1021/acs.jpcb.4c05368, 10.1016/j.cap.2018.07.011, 10.1021/acs.macromol.5c00158, 10.1080/07391102.2018.1541762). Did the authors compare their results with these works? We appreciate the reviewer's input and the suggested literature. However, because those works address copolymer chains and polymer blends, their findings are not directly applicable or comparable to the behavior of the homopolymer systems investigated in our manuscript. *-Since CG models often deviate from experimental values due to the absence of detailed atomistic interactions, how did the authors address this limitation in their parameterization?* We understand the Reviewer's concern regarding potential deviations from experimental values in coarse-grained (CG) models. We addressed this limitation by implementing a systematic parameterization approach where the CG interaction potentials were derived directly from high-quality atomistic simulations. This rigorous methodology guarantees the CG model inherently reproduces the structural properties (i.e., structural fidelity) of the reference atomistic system, ensuring the underlying physics is preserved. The reliability of our CG results stems from the accuracy of the atomistic model, which utilizes the advanced force field capable of quantitatively describing the system's properties. Our atomistic model has been thoroughly validated against existing simulation literature. We note that a direct, quantitative comparison to experimental data is not generally feasible for our specific system (monodisperse amorphous PCL at the studied molecular weight) because available experimental results are often biased by factors like crystallinity and polydispersity. However, for properties where a qualitative or semi-quantitative comparison is appropriate despite these limitations, we did include experimental data: specifically, we compare our results with rheological measurements in the final section of the manuscript. As noted in that section, this comparison is made with a discussion of the above-mentioned limitations. *-If the purpose of CG was to access larger chain lengths, did the authors also perform simulations of higher molecular weight PCLs to test the robustness of the model?* As confirmed by Figure 9, the longest polymer chain investigated in our work approaches the limit of the entangled regime. A thorough, quantitative study of fully entangled systems requires a substantially more intensive equilibration process and greater computational resources. Consequently, the detailed analysis of the dynamics within the fully entangled regime is beyond the scope of the current article and will be the focus of future work.

1. *If the entire monomer was mapped as a single bead, how were polarization effects and hydrogen-bond interactions from polar atoms accounted for in the CG model? Please clarify whether effective interactions were adjusted for this purpose.*

Given the inherent simplifications of our coarse-grained model, polarization effects were not explicitly included. Regarding hydrogen bonds, the simulation temperature is high and the potential donor groups are present solely at the polymer chain ends. Because these

conditions severely limit the formation and stability of H-bonds, making their effect minor, we judged their explicit inclusion unnecessary for accurate structural reproduction and thus omitted them from the coarse-grained representation. Nevertheless, for systems studied at lower temperatures, additional effective CG interactions accounting for hydrogen bonding could be incorporated, and this will be explored in future work.

1. *The authors should clearly define how the monomer-to-monomer bond lengths, angles, and dihedrals were calculated. Were these distributions directly obtained from AA simulations, or were they imposed during the IBI process?*

We extended the discussion related to the IBI procedure. The bond, angle, dihedral distributions as well as the radial distribution function were first calculated from the atomistic simulations (Figure 2 in the manuscript). Then the target atomistic distributions were converted into initial estimates of the potentials through direct Boltzmann inversion. In continuation, the IBI process was applied to refine the coarse-grained potentials.

1. *The reported CG densities show deviations compared to the all-atom model, even though the parameters were derived from AA simulations. Could the authors explain why this discrepancy occurs and what might be the source of such variation?*

Even though there are some discrepancies in the average values (only around 1%), for the vast majority of systems the coarse-grained densities fall within the calculated error bars of the atomistic data. A minor exception was observed only for the PCL50 system, which exhibited a slight deviation outside this range. Given the good agreement observed across the full set of molecular weights, we consider the systematic coarse-graining procedure to be successful in reproducing the target properties.

Competing Interests: No competing interests were disclosed.